Cooperative Hydrogen Bonds of Macromolecules. 2. Two-Dimensional Cooperativity in the Binding of Poly(4-vinylpyridine) to Poly(4-vinylphenol)

Jaroslav Kříž,* Jiří Dybal, and Jiří Brus

Institute of Macromolecular Chemistry, Academy of Sciences of the Czech Republic, Heyrovsky Square 2, 162 06 Prague 6, Czech Republic

Received: June 20, 2006; In Final Form: July 25, 2006

The hydrogen bond interaction of poly(4-vinylphenol) (PVF), ligated by a 20 mol/mol excess of pyridine-d_5 (PD) in tetrahydrofuran-d_8, with poly(4-vinylpyridine) (PVP) was studied using liquid and solid-state NMR and quantum mechanical calculations. Because of its cooperative interaction, PVP substitutes PD in its hydrogen bond with PVF, thus forming a PVF−PVP complex, which gradually precipitates from solution. On the basis of the ^{1}H/^{13}C NMR spin-diffusion experiments and density functional theory quantum calculations, the complex is shown to have the fairly regular structure of a polymer sheet with intermittent H-bond links between PVF and PVP chains. The cooperativity of PVP interaction with PVF was studied by measuring the dependence of the binding degree α of PVP on its polymerization degree (P_n, being 10, 17, 30, 36, 48, 65, and 84) at various PVP/PVF molar ratios. The value of α was established indirectly by measuring the fraction of liberated PD using its ^{2}H quadrupolar relaxation and pulsed field-gradient spin−echo measurement of self-diffusion. The cooperativity is shown to be of a higher order and two-dimensional, that is, dependent on both the polymerization degree of PVP and its ratio to PVF. A mathematical model of such two-dimensional cooperativity based chiefly on a proximity effect is suggested.

Introduction

Cooperative electrostatic, hydrogen bond (H-bond), or hydrophobic interactions have been recognized as being crucial for the formation of natural or synthetic macromolecular complexes,[1−4] in particular those that are endowed with some specific function. Although hundreds or more individual examples of such cooperative binding have been recognized and studied (for H-bonds, see, e.g., refs 5−23), little systematic work has been done in this field except on the study of cooperative electrostatic interactions[24−30] between oppositely charged macromolecules. It became clear in these studies that the cooperation of binding could be of a linear (first-order) or nonlinear (higher-order) kind. Expressed quantitatively, the overall change in the Gibbs energy of binding of two macromolecules can be partitioned into contributions from the individual pairs of complementary groups, $\Delta G_i^{(1)}$, and additional contributions from doubles, $\Delta G_{ij}^{(2)}$, triples, $\Delta G_{ijk}^{(3)}$, and so forth, of such pairs:

$$\Delta G = \sum_{i=1}^{n} \Delta G_i^{(1)} + \sum_{i=1}^{n-1} \sum_{j=i+1}^{n} \Delta G_{ij}^{(2)} + \sum_{i=1}^{n-2} \sum_{j=i+1}^{n-1} \sum_{k=j+1}^{n} \Delta G_{ijk}^{(3)} + \ldots$$

The binding is cooperative, even if most of the higher sums vanish, providing that most of the terms in the first sum are negative. Such a case can be dubbed first-order cooperation. It can be shown to ensure progressively stronger binding with an increasing number of binding sites in the macromolecule, but this change is not dramatic. Although this type of cooperation is widely assumed to be the usual one, it actually appears to be rather rare, at least in the case of Coulomb electrostatic interactions. The reason usually is that the first-order terms tend to be slightly positive as a result of, for example, steric hindrances. The cooperation of binding is then provided for by the higher-order terms. The typical dependence of the binding degree α on the number of binding sites *n* in such a case has a sigmoidal shape with a steep rise after some critical *n* and a convergent behavior for large values of *n*. In such a case of higher-order cooperative binding, three main factors were found: (i) entropy gained by liberation of small ligands (ions, interacting solvent molecules) originally bound to the binding sites by a nonlinear collective force (e.g., the so-called polyelectrolyte effect in the case of small ions); (ii) collision statistics of the reactant groups perturbed by the already formed bonds in the complex (proximity effect);[30] (iii) hydrophobic interactions and other collective less specific pseudo-phase effects.

It is highly probable that at least some of these factors are also important in the cooperative hydrogen bindings of macromolecules, which are much more prevalent in the self-assembly of functional complexes both in nature and synthetic nanotechnology.

In this study, we examine the cooperative binding between poly(4-vinylphenol) (PVF) as a polymer H-bond donor and poly(4-vinylpyridine) (PVP) as an H-bond acceptor. To demonstrate the cooperativity of binding between PVF and PVP, we use PVF primarily hydrogen-bonded to pyridine, a low-molecular-weight analogue of PVP. This also makes it possible for us to quantitatively estimate the binding degree between PVF and PVP in light of the dependence on the chain length of the latter by measuring the degree of liberation of pyridine using a method described in our previous study.[37]

Experimental Section

1. Materials. PVF with $M_n = 10\,000$ was purchased from Interscience. Defined samples of PVP with $M_n = 1000$, 1760,

* To whom correspondence should be addressed. E-mail: kriz@imc.cas.cz. Phone: +420-296809382. Fax: +420-296809410.

10.1021/jp063837a CCC: $33.50
Published on Web 08/24/2006

3200, 3800, 5100, 6800, and 8800 ($M_w/M_n < 1.2$) were purchased from Polymer Source, Inc. Tetrahydrofuran-d_8 (TDF), pyridine-d_5 (PD) and chloroform-*d* were obtained from Aldrich and were held over a molecular sieve before use.

2. Preparation of Samples. Solution A: 72.1 mg (0.6 meq OH) of PVF was dissolved in a mixture of 1.0 mL of PD (12.46 mmol), 4.4 mL of TDF and 0.6 mL of chloroform-*d*. Solution B: 42.1 mg (0.4 meq) of PVP was dissolved in 4.0 mL of TDF. Samples for NMR: 1.0 mL of A plus $(1 - x)$ mL of TDF was put into a vigorously magnetically stirred bottle, and x mL ($x = 0.2$, 0.4, 0.6, 0.8, and 1.0) of B was added by a syringe pump at a rate of 0.02 mL/min. Immediately after mixing, 0.6 mL of the mixture was transferred into an NMR tube, which was sealed. For quantitative estimation of the binding degree of PVF with PVD, the samples were stored for at least 24 h at room temperature, and the precipitate of the PVF−PVD complex was removed from the measuring area by centrifugation (1 h at 6000 rev/min).

For preparation of the PVF−PVP complex, 105.13 mg (1 meq) of PVP ($M_n = 8800$) in 10 mL of tetrahydrofuran (THF) was slowly added under magnetic stirring to a solution of 120.15 mg (1 meq) of PVF ($M_n = 10\,000$) in 10 mL of THF. The mixture was stored for 24 h, then the precipitate was isolated by centrifugation, washed twice with THF, and dried for 48 h under vacuum.

3. Liquid-State NMR Measurements. ^{1}H and ^{2}H NMR spectroscopic, relaxation, and pulsed field-gradient (PFG) measurements were done with a Bruker Avance DPX300 spectrometer using a *z*-gradient inverse-detection multinuclear probe (^{1}H spectra and ^{2}H PFG) and a multinuclear broadband probe (^{2}H relaxations). ^{2}H measurements were done without lock, each of them being repeated at least five times with the resulting quantities (T_1 or D_s) fluctuating at most ±3% rel. Longitudinal (T_1) ^{2}H NMR relaxations were measured using the conventional inverse-recovery pulse sequence d_1-π-υd-π/2-FID, with υd being variable delay, collecting 32 scans for 16 points. PFG spin−echo (PGSE) self-diffusion time measurements were done on the ^{2}H resonance using the Stejskal−Tanner[31] sequence, d_1-π/2-Gr-d_2/2-π-d_2-Gr-FID (Gr meaning gradient pulse), with d_2 being fixed at a 200 ms value and the power of the 2 ms *z*-gradient pulse being varied from 0 to 50 G/cm in 16 increments. The magnitude of the self-diffusion coefficient of PVF was measured on a special water-cooled PFG ^{1}H probe using the Tanner[32] stimulated echo sequence (PGSTE) d_1-π/2-Gr-π/2-d_2-π/2-Gr-FID, with fixed $d_2 = 40$ ms and 1 ms *z*-gradient pulses varied from 0 to 720 G/cm in 16 increments. The decay curve was fitted with three exponential functions in this case, and a weighted mean of their respective constants was taken as the diffusion coefficient.[37]

4. Solid-State NMR. All NMR spectra were measured with a Bruker Avance 500 NMR spectrometer (Karlsruhe, Germany, 2003) in a 4 mm ZrO_2 rotor. The magic-angle spinning (MAS) speed was 11 kHz in all cases, the nutation frequency of the B_1(^{13}C) field for cross-polarization (CP) was 62.5 kHz, and the repetition delay was 2−4 s. For recording of the ^{1}H−^{13}C HETCOR spectra,[33,34] a frequency-switched Lee−Goldburg (FSLG) decoupling field strength of $\omega_1/2\pi = 100$ kHz was applied during an indirect detection t_1 period consisting of 128 increments, each made of 320 scans. On-resonance CPs ranging from 0.1 to 5.0 ms were used as a mixing period. The intensity of the B_1(^{1}H) field for CP was $\omega_1/2\pi = 62.5$ kHz. Two-pulse phase-modulated (TPPM) decoupling[35] was applied during the detection of the ^{13}C NMR signal. The phase modulation angle was 15°, and the flip-pulse length was 4.8 μs. The applied nutation frequency of the B_1(^{1}H) field was $\omega_1/2\pi = 89.3$ kHz. The ^{13}C scale was calibrated with glycine as an external standard (176.03 ppm; low-field carbonyl signal). The external standard L-[U-^{13}C,^{15}N] Ala was used for calibration of the ^{1}H scale. The ^{1}H chemical shift of Hβ was set to 1 ppm, and the proton chemical shift scale was corrected to achieve the ^{1}H chemical shift of Hα and NH_3^+ signals of ∼3.8 and 9.2 ppm, respectively.

5. Quantum Mechanical Calculations. The model structures modeling the PVF−PVP complex were simulated by density functional theory (DFT) (B3LYP/3-21G(d) for two hexamers of PVP and PVF) and ab initio self-consistent field (SCF) (HF/STO-3G for four octamers) methods using the Gaussian program package.[36] The optimization of the geometries was unrestrained in the quest for the global energy minimum.

Results

1. Observation of PVF−PVP Interaction and Characterization of the Resulting Complex. In the experiments, a 0.1 mol/L solution of PVP in TDF was slowly added to a 0.1 mol/L solution of PVF in a mixture of TDF, PD, and $CDCl_3$. The molar ratio of PD to OH groups of PVF was 20.77. Because the equilibrium constant of PD hydrogen bonding to PVF in TDF is[37] approximately 5.3 mol^{-1} L^{-1}, 99.5% of the hydroxyl groups of PVF are initially occupied by PD. Despite this, visible clouding of the mixture by the PVF−PVP complex is observed during PVP addition, particularly in the case of longer-chain PVP. The number-mean polymerization degrees (P_n) of PVP were approximately 10, 17, 30, 36, 48, 65, and 84. For the first two, clouding of the originally clear solution visibly appeared after reaching the ratio $\beta = 0.4$ mol/mol (PVP/PVF), whereas it already started with the first additions of the last two polymers. ^{1}H NMR shows a relative integral intensity decrease and broadening of both PVF and PVP signals but little change in their positions. Repeated observation of the same sample in intervals of 2 h showed further broadening and intensity decrease of the signals. At the same time, the clouding deepened, and a white precipitate slowly appeared on the bottom of the tube. In all cases, these changes ended in 24 h. After this time, most of the precipitate was removed from the observation zone by centrifugation, leaving an opalescent or slightly clouded supernatant. This operation did not significantly change the intensity of the remaining NMR signals, thus showing that the signals of the coagulated product are invisible due to extreme broadening. Thus, the mobility of the product must be severely restricted.

In Figure 1, ^{1}H NMR spectra of some of the samples with different P_n of PVP ($\beta = 1.0$ in all cases) after centrifugation are shown. Clearly, the extent of immobilized and removed product increases upon increasing the polymerization degree of PVP, thus suggesting that the cooperativity of its bonding to PVF depends on its chain length. However, the intensity decrease, even at $P_n \approx 10$, is about 40% rel, which shows substantial cooperativity considering the 20 molar excess of pyridine, which must be substituted in PVP bonding.

The fact that the remaining signals of both PVF and PVP are narrower for short PVP oligomers suggests that a part of the product could still be visible in liquid-state NMR. Therefore, the intensity of the ^{1}H NMR signals is not quite a reliable measure of the extent of PVF−PVP bonding. This is provided for by measuring the extent of liberated PD, which is reported in another section of this paper.

For its characterization, the PVF−PVP complex was prepared in a larger amount by mixing equal amounts of 0.1 mol/L THF solutions of PVF ($M_n = 10\,000$) and PVP ($M_n = 8800$) and isolating the product. According to wide-angle X-ray scattering,

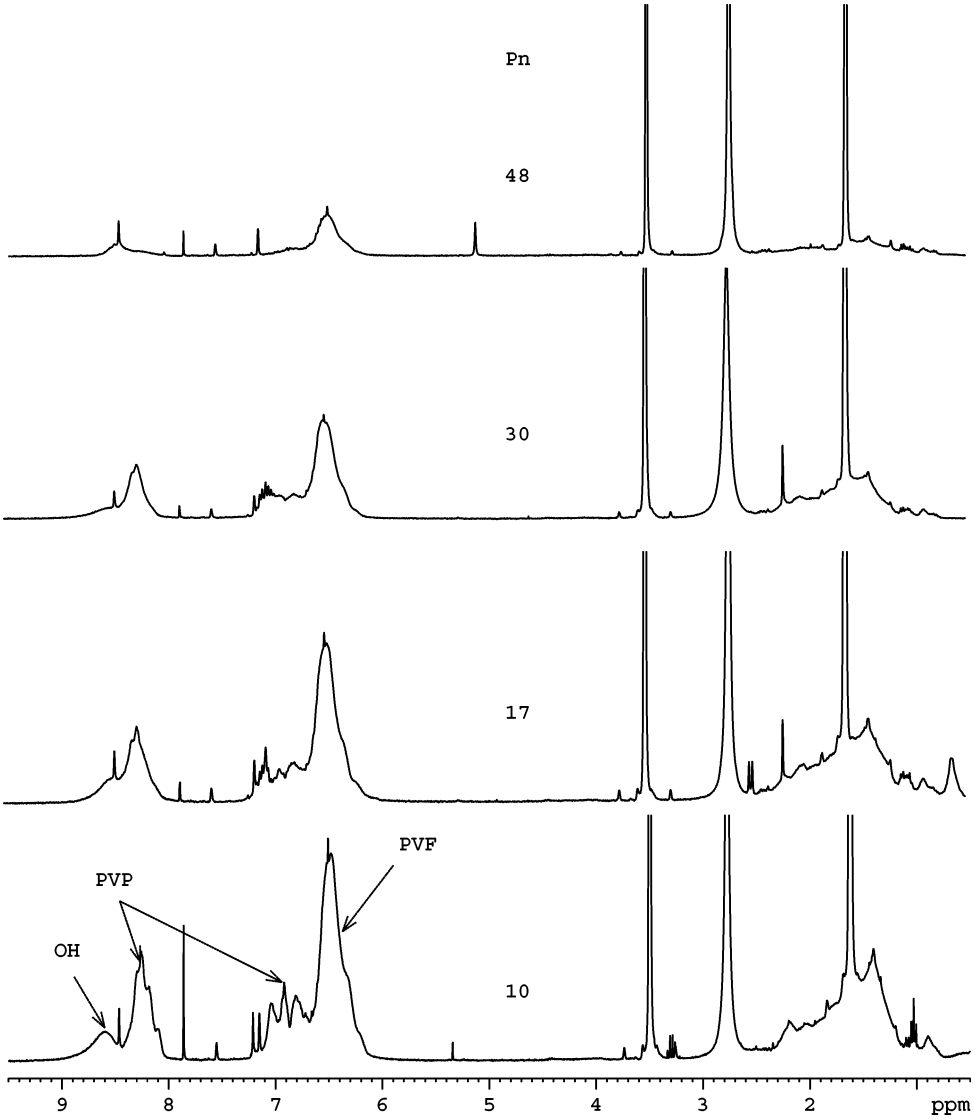

Figure 1. Liquid-state ^{1}H NMR spectra of the 1:1 mixtures of 0.1 mol/L solutions of PVF and PVD in PD/TDF solutions after centrifugation (298 K)

the complex has a virtually amorphous nature, which could be expected considering that both polymers were atactic (although with predominant syndiotactic dyads) and not exactly matching in polymerization degree.

More specific information about the complex was provided by solid-state NMR. The simple comparison of the ^{13}C CP/MAS NMR spectra of neat PVP, PVF, and their complex in Figure 2 confirms the presence of a mutual interaction between both polymer components. This interaction induces significant changes in the resonance frequencies of the interacting structure units, predominantly in ═**C**−OH (PVF) and ═**C**H−N− (PVP). While the signal of para carbon ═**C**H−OH is downfield shifted about 1.6 ppm, that of ═**C**H−N− carbon is upfield shifted about 0.8 ppm. This clearly reflects changes in the distribution of electron density, which is caused by the formation of hydrogen bonds between the hydrogen bond donor and acceptor. No additional broadening of NMR signals of both components in the polymer complex is observed, which indicates a high extent of hydrogen bonding and a relatively regular arrangement of both types of macromolecules within the system.

Additional information about the structure is provided by spin-diffusion experiments. The two-dimensional ^{1}H−^{13}C HETCOR technique nicely combines the advantage of ^{1}H nuclei (100% isotopic abundance and high magnetogyric constant, allowing observation of the spin diffusion and thus providing geometrical constraints) with the high resolution of ^{13}C NMR spectra. In this experiment, ^{1}H−^{1}H spin exchange occurs during the mixing period of on-resonance CP. In the resulting spectra (Figure 3), we observe two types of correlation signals. At a very short mixing period, virtually only signals reflecting the shortest (usually one-bond) ^{1}H−^{13}C spin pairs occur. At longer mixing times, additional cross-peaks gradually occur, reflecting long-range through-space polarization transfer, that is, long-range interatomic contacts. The latter signals can be used to estimate the geometry of the studied system. For a short mixing time of t_m = 100−300 μs, cross-peaks for only directly bonded ^{1}H−^{13}C pairs and the shortest intraresidual contacts evolve in our case. From these, we were able to identify ^{1}H NMR signals of protons in structure units involved in mutual interaction of polymer chains (═C−O**H** and ═C**H**−N− at 8.1 and 9.8 ppm, respectively). The extraordinary position of the ^{1}H NMR signal of ═C**H**−N− in PVP makes it possible to probe its average distance to the ═C−OH carbon in PVF. A corresponding ^{1}H/^{13}C correlation signal of ═C**H**−N−/═**C**−OH reflecting intermolecular contact was clearly detected after 500 μs, while full equilibration was reached within 0.8 ms. This confirms a high extent of mutual interaction via hydrogen bonds. Using the

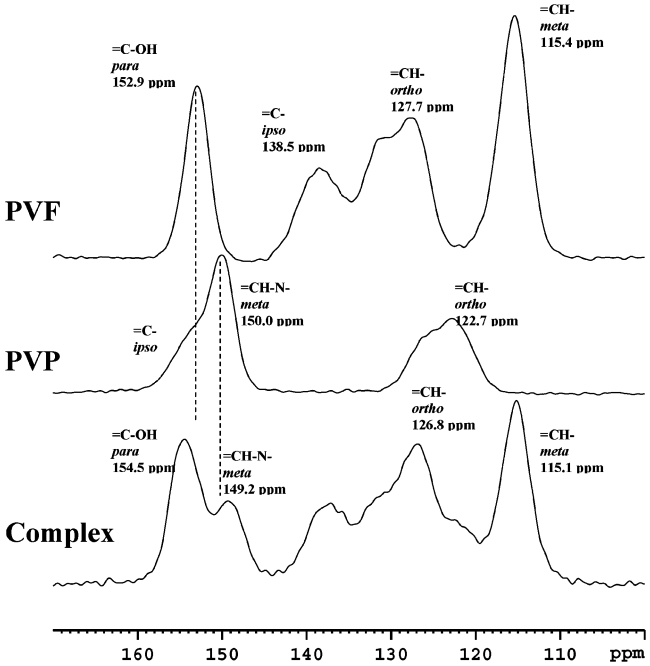

Figure 2. Expanded region of the ^{13}C CP/MAS NMR spectra of PVF, PVP, and their complex.

simplest equation describing spin diffusion,[38,39] $x = 2\epsilon\sqrt{Dt_{eq}/\pi}$ (where x is the length of the spin-diffusion pathway, ϵ is the dimensionality of the process, D is the spin-diffusion coefficient, and t_{eq} is the time, after equilibrium is reached), we tried to estimate the length of the polarization transfer pathway from the =C**H**−N− proton to the =**C**−OH carbon, which can be simply considered to be an average distance between the respective nuclei. For rigid polymer systems, the value of the spin-diffusion coefficient $D = 0.6 \times 10^{-15}$ m^2 s^{-1} is generally acceptable, and the dimensionality of this process in a system with simple morphology is usually $\epsilon = 1$. Taking into account that the spin-diffusion process in spin-lock during CP is slowed to one-half and using the limiting values of mixing times (0.5 and 0.8 ms), the resulting interatomic distance is 0.4−0.5 nm.

The obtained distance is in very good agreement with the structure of the PVF−PVP complex optimized by high-precision quantum calculation (see below), predicting the distances between the two C**H**=N protons and =**C**−OH to be equal to 0. 378 and 0.486 nm, respectively. These values suggest strong and uniform hydrogen bonding between the two polymers and, consequently, a rather uniform structure of the complex.

2. Quantum Mechanical Calculations on the PVF−PVP Complex. The prediction of the most probable structure of a polymer complex by theoretical calculation meets the well-known obstacle that computational methods with reliable accuracy (such as ab initio−DFT with a sufficient basis set of atomic orbitals) are practically feasible for relatively low-molecular-weight systems. On the other hand, methods tolerating larger systems are usually less reliable. Therefore, we proceeded in two steps. First, we sought the optimal geometry for two interacting hexamers of PVF and PVP using the highly reliable DFT method with the B3LYP/3-21G(d) basis set. In this as well as in the second step, we assumed that both oligomeric types have syndiotactic structure. One of the two resulting optimal geometries found by our calculations is shown in Figure 4. In this structure, only half of the hydrogen bond donor and acceptor groups are coupled, whereas the other half remain free for further bonding. This structure is free of any steric strain and is a probable structural motif of a more extensive molecular system.

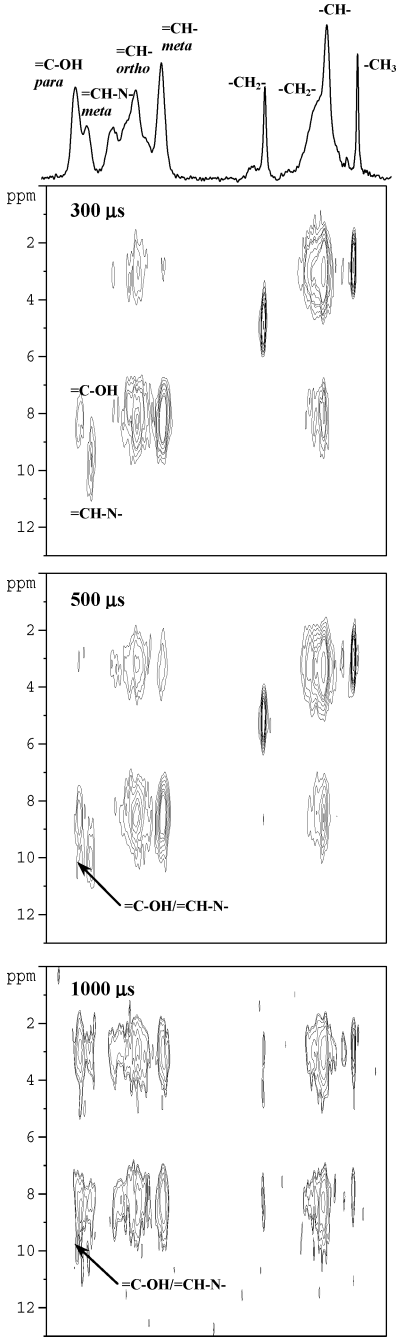

Figure 3. Two-dimensional $^1H-^{13}C$ HETCOR (500 MHz) spectra of the polymer complex obtained with spin-diffusion mixing times of t_m = 300, 500, and 1000 μs.

In addition to this geometry, the calculation found another one with a ladder-like structure in which all donor and acceptor groups are coupled in pairs. This second structure actually has a somewhat lower predicted energy due to the three additional hydrogen bonds but has a skewed geometry with substantial steric strain, which makes its more extended version improbable.

In the second step, we calculated the optimum structure of a system of two PVF and two PVP octamers using a less accurate ab initio SCF method with an STO-3G basis set. The optimal structure shown in Figure 5 has almost identical structural motifs, as predicted by the DFT calculation above. It shows that hydrogen bonds between PVF and PVP chains can be formed without strain in the natural conformation of the chains, that is, with the aromatic rings in almost trans position to each other. In the structure, H-bonds intermittently bind two neigh-

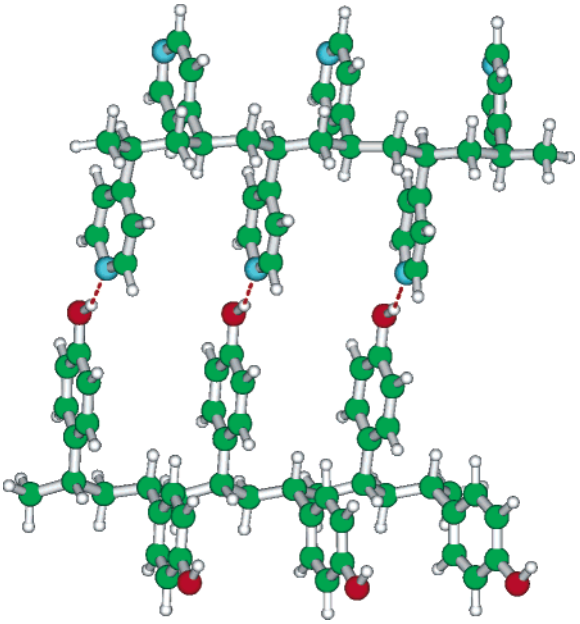

Figure 4. Optimal structure of the complex of two PVF and PVP hexamers predicted by the ab initio−DFT method with the B3LYP/3-21G(d) basis set.

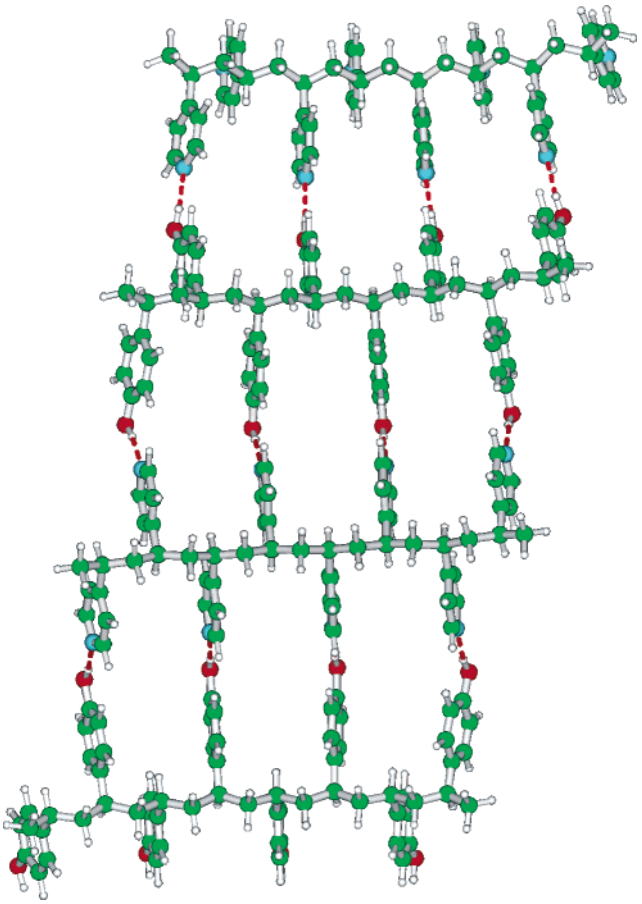

Figure 5. Optimal geometry of a system of four interacting PVF and PVP octamers predicted by ab initio SCF (HF/STO-3G) calculation.

boring chains, thus forming a polymer sheet with a mean width depending on the PVP/PVF ratio (spanning only three chains for 2/1 and theoretically infinite for 1/1).

The polymer sheet structure suggested in Figure 5 is in semiquantitative agreement with the results of solid-state NMR (see above). In reality, it is prone to have various imperfections given, for example, by the fact that our polymers are atactic rather than purely syndiotactic. However, it explains the rather strong dependence of the binding degree of PVP on its ratio to PVF (see below).

3. Quantitative Measurements of the Cooperativity in PVF−PVP Interaction. The mere fact that PVP binds to PVF even under 20 mol/mol excess of pyridine clearly shows that this interaction must be cooperative. For quantification of this cooperativity, there probably is only one precise tool, namely, measuring the extent of pyridine liberated due to its substitution by the pyridine units of PVP. As shown in our previous study,[37] this can be done (under the condition of fast exchange between the free and bound pyridine) by measuring either the deuterium quadrupolar relaxation rate or the self-diffusion coefficient of PD in the system. The molar fraction φ of PD still bound to PVF can be calculated from the relation

$$\varphi = \frac{R_1^N - R_{1F}^N}{R_{1B}^N - R_{1F}^N} \tag{1}$$

where R_1, R_{1B}, and R_{1F} are the relaxation rates measured in the actual system and in the bound and free states, respectively, and the superscript N means normalization to a standard viscosity[37] using the relaxation rate of some inert component such as $CDCl_3$. Alternatively, φ can be calculated from

$$\varphi = \frac{D_F^N - D^N}{D_F^N - D_B^N} \tag{2}$$

where D, D_F, and D_B are the self-diffusion coefficients of PD in the system and in the bound and free states, respectively, and the superscript N has the same meaning as above. From φ, the fraction α of the groups of PVP bound to PVF can be obtained by the relation

$$\alpha = \frac{(\varphi_0 - \varphi)[PD]_0}{[VP]_0} = \frac{(\varphi_0 - \varphi)\psi}{\beta} \tag{3}$$

where $[PD]_0$, $[VP]_0$, and $[VF]_0$ are the initial concentrations of PD and the vinylpyridine and vinylphenol groups, respectively, $\beta = [VP]_0/[VF]_0$, and $\psi = [PD]_0/[VF]_0$.

In all experiments reported here, the value of $[VF]_0$ was 0.1 eq/L, and that of ψ was 20.77. The experiments were carried out by adding a TDF solution of the given PVP ($[VP]_0 = 0.1$ eq/L) to a TDF solution containing PVF, PD, and $CDCl_3$ (for details, see Experimental Section) at 298 K. Both ^2H NMR longitudinal relaxations and PGSE diffusion measurements were done at 300 K. As shown in our previous study[37] and verified here, the exchange of PD between its bound and free state is fast enough at 300 K to ensure a purely monoexponential decrease of signal intensity that is dependent on time (relaxation) or on the square of the pulsed field gradient (PGSE) so that the evaluation of R_1 or D used in eqs 1 and 2 is straightforward.

A high value of ψ was needed to suppress the competition of TDF in primary binding to PVF but is very demanding with respect to the precision of both relaxation and diffusion experiments because the values of R_1^N or D^N vary only slightly due to a large excess of free PD. Therefore, each of these values was measured five or more times to ensure a variation of less than 3% rel. The results of the experiments are given in Table 1. For illustration, the dependences of α on P_n are shown in Figure 6. They clearly have a sigmoidal shape, indicating higher-order cooperativity in the sense explained in the Introduction.

TABLE 1: Normalized Relaxation Rates R_1^N (γ-D) and Self-Diffusion Coefficients D^N of PD and the Resulting Calculated Binding Degrees of the Three Shortest Oligomers of PVP in Their Mixtures with PVF, PD, and TDF[a]

P_n	β mol/mol	R_1^N s^{-1}	φ mol/mol	α eq/eq	$D^N \times 10^9$ $m^2\ s^{-1}$	φ mol/mol	α eq/eq	α_{mean} eq/eq
10	0.2	3.450	0.0482	0.145	1.723	0.0483	0.134	0.140
	0.4	3.342	0.0460	0.184	1.726	0.0462	0.173	0.179
	0.6	3.103	0.0411	0.285	1.734	0.0414	0.274	0.279
	0.8	2.824	0.0354	0.355	1.743	0.0359	0.343	0.349
	1.0	2.555	0.0299	0.394	1.751	0.0306	0.382	0.388
17	0.2	3.450	0.0482	0.149	1.723	0.0482	0.140	0.144
	0.4	3.337	0.0459	0.189	1.726	0.0460	0.180	0.185
	0.6	3.088	0.0408	0.294	1.734	0.0411	0.284	0.289
	0.8	2.804	0.0350	0.366	1.743	0.0354	0.356	0.361
	1.0	2.525	0.0293	0.406	1.752	0.0299	0.396	0.401
30	0.2	3.440	0.0480	0.164	1.723	0.0481	0.156	0.160
	0.4	3.318	0.0455	0.209	1.726	0.0457	0.200	0.205
	0.6	3.044	0.0399	0.326	1.736	0.0402	0.315	0.320
	0.8	2.726	0.0334	0.406	1.746	0.0338	0.395	0.400
	1.0	2.423	0.0272	0.450	1.755	0.0277	0.440	0.445
36	0.2	3.430	0.0478	0.184	1.723	0.0479	0.176	0.180
	0.4	3.292	0.0450	0.234	1.728	0.0451	0.226	0.230
	0.6	2.987	0.0387	0.364	1.738	0.0390	0.355	0.360
	0.8	2.633	0.0315	0.454	1.749	0.0319	0.445	0.450
	1.0	2.313	0.0250	0.494	1.760	0.0249	0.495	0.495
48	0.2	3.395	0.0471	0.257	1.725	0.0472	0.248	0.252
	0.4	3.201	0.0431	0.327	1.731	0.0432	0.318	0.323
	0.6	2.774	0.0344	0.509	1.745	0.0347	0.500	0.505
	0.8	2.276	0.0242	0.636	1.761	0.0246	0.626	0.631
	1.0	1.794	0.0143	0.706	1.776	0.0149	0.696	0.701
65	0.2	3.351	0.0462	0.348	1.725	0.0466	0.302	0.325
	0.4	3.095	0.0410	0.435	1.733	0.0417	0.395	0.415
	0.6	2.532	0.0294	0.674	1.751	0.0309	0.625	0.649
	0.8	1.889	0.0163	0.834	1.771	0.0181	0.790	0.812
	1.0	1.261	0.0035	0.924	1.791	0.0057	0.880	0.902
84	0.2	3.351	0.0462	0.347	1.726	0.0463	0.340	0.344
	0.4	3.086	0.0408	0.444	1.735	0.0410	0.435	0.439
	0.6	2.504	0.0289	0.693	1.753	0.0292	0.682	0.688
	0.8	1.828	0.0151	0.865	1.775	0.0155	0.854	0.860
	1.0	1.175	0.002	0.959	1.797	0.002	0.950	0.955

[a] $R_{1F}^N = 1.092\ s^{-1}$; $R_{1B}^N = 50.01\ s^{-1}$; $D_F^N = 1.800 \times 10^{-9}\ m^2\ s^{-1}$; $D_B^N = (1.282-2.019) \times 10^{-10}\ m^2\ s^{-1}$.

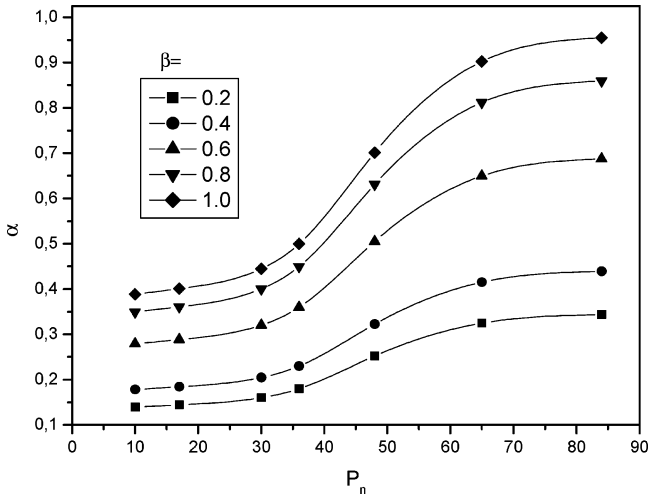

Figure 6. Dependence of the binding degree of PVP in its interaction with PVF on its polymerization degree under the indicated ratio $\beta = [VP]_0/[VF]_0$.

In addition to the cooperativity depending on P_n, we observe a somewhat less pronounced but still perceptible one depending on β, that is, on the $[PVP]_0/[PVF]_0$ ratio, as illustrated in Figure 7. This cooperativity can be said to operate in a second dimension, so that, as a whole, we can consider the cooperativity in the PVF−PVP interaction as being *two-dimensional*.

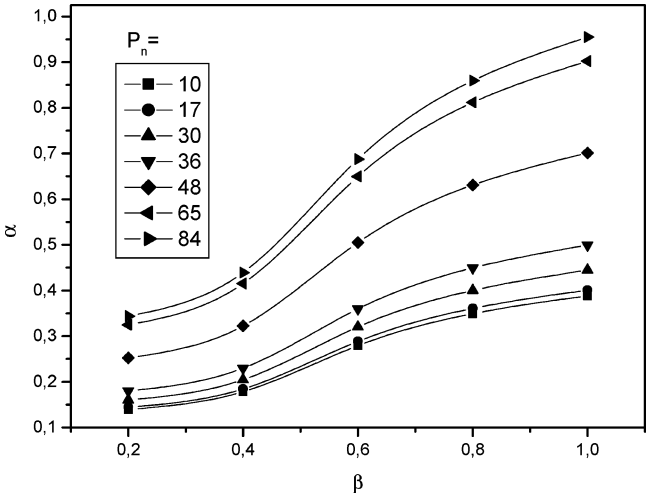

Figure 7. Dependence of the binding degree of PVP of various polymerization degrees (indicated in the Figure) on the ratio β.

Discussion

1. The Nature of the Cooperativity Observed. In the last part of the Results, we demonstrated that the binding of PVP to PVF is clearly cooperative: (i) the binding is effective, even under the 20 mol/mol excess of pyridine competing with PVP; (ii) the dependence of the binding degree α on the polymerization degree P_n of PVP as well as on the [VP/VF] ratio β is sigmoidal. From (ii), we can infer that the cooperativity observed is of a higher order and operates in two dimensions.

There could be two main reasons for cooperativity in PVF−PVP binding. First, there is a gain in entropy of the originally bound pyridine due to its liberation by the binding groups of PVP, which must be substantially larger than the complementary loss of entropy of PVP groups. However, this factor can scarcely be decisive for a cooperativity nonlinearly dependent on the chain length of PVP.

This invokes the second and more probable cause, namely the *proximity effect* already introduced[30] in connection with the coupling of weakly charged complementary polyions. This principle is based on the fact that a bond already accomplished between two polymers strongly reduces the effective volume in which the neighboring reactant groups can move relative to each other, shifting thus their effective equilibrium constant of binding to a much higher value. In one of our previous studies,[30] we showed that even the equilibrium of coupling two independent molecules, A and B, into an adduct, AB, is shifted to a higher level if the relative motion of A and B is confined in a restricted volume, the reason being a change in the translation partition function. In the case of two interacting polymer chains, the already accomplished bonds restrict both the relative translation and rotation (conformation) motions of the nearer reactant groups to the same effect. From the point of view of thermodynamics, it is an *entropy* effect due to the fact that the variety of translations and rotations (in other words, relative positions and conformations) is restricted by the already accomplished bonds.

As the coupled pair of polymers gets progressively tougher with each accomplished bond between them, the resulting cooperativity is nonlinear. In our case, this is probably the main source of cooperativity in the *first dimension*, that is, of the strong dependence of α on the chain length of PVP. To interpret the cooperativity in the *second dimension*, that is, the weaker but still perceptible dependence of α on the [VP]/[VF] ratio β, we have to first recall the most probable structure of the PVF−

SCHEME 1

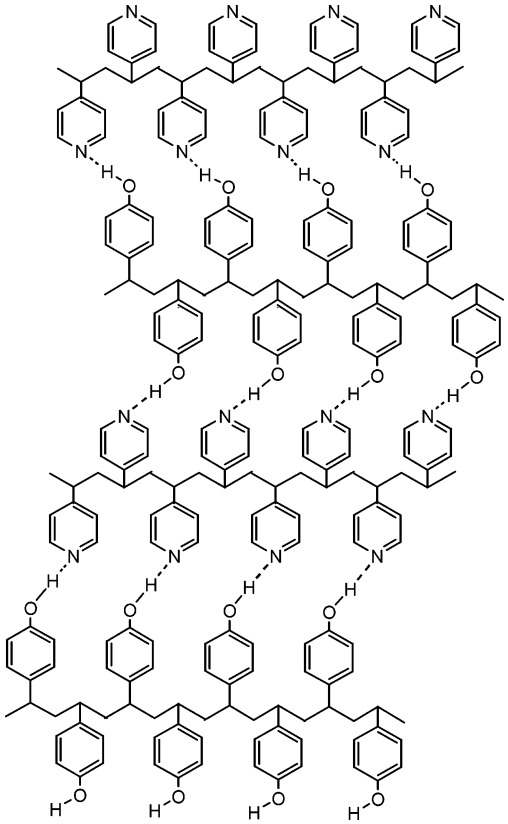

PVP complex as suggested by both solid-state NMR and quantum calculations, namely, the regular two-dimensional sheet illustrated in Scheme 1.

In forming such a scheme, the efficiency of building-up the next row of the sheet, for example, from left to right, depends not only on the number of links already accomplished on the left side but also on the rigidity of the complex to which the incident polymer is being attached. Up to some limit, the rigidity will increase with the increasing width of the sheet. An elementary consideration will show that the resulting width of the sheet increases with increasing β, theoretically reaching infinity at $\beta = 1.0$. The main ideas of this interpretation are expressed more quantitatively in the following section.

Rather surprisingly, values of α over 0.92 (or near to unity) were reached in some cases. This indicates rather perfect matching of the interacting polymers, which is not very probable. As α is determined indirectly by measuring the extent of freed pyridine, we cannot be quite sure that some other mechanism does not lead to some over-estimation of its value.

2. Mathematical Model of Two-Dimensional Cooperativity. Let us have two homopolymers with monomer units A (hydrogen bond acceptor) and B (hydrogen bond donor), which, for steric reasons, bind alternately in the manner shown in Scheme 2 (the scheme shows only half of the process). If each binding step is an equilibrium process, the end result does not depend on the path. Therefore, we are allowed to describe the consecutive binding as if going regularly from left to right and then to the subsequent row as indicated in Scheme 1. We assume that the first binding in each row corresponds to a simple equilibrium with a constant K. All next steps in the same row have another equilibrium constant K_1 and are affected by the proximity effect[30] of an already existing binding expressed by a factor ξ_k for the kth consecutive step (first-dimension cooperativity). Additionally, for each next row of binding, we

SCHEME 2

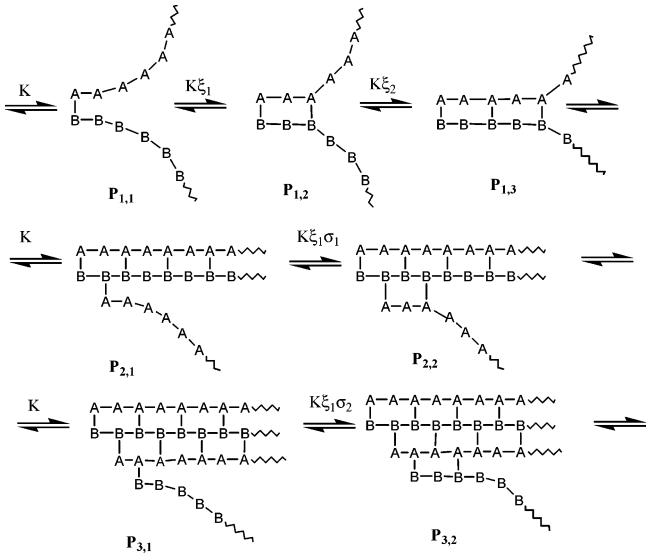

assume another factor σ_j expressing the benefit of already formed j rows of bonds (second-dimension cooperativity). The rationality of these assumptions is based on the following brief arguments. In the first dimension, the already accomplished links between the polymer chains decrease the effective volume, in which the remaining groups A and B can move. As already explained in one of our previous studies,[30] this changes the probability of their encounter in a similar way as if their local concentration were steeply increased. In the second dimension, the additional effect is given by the fact that the structure bearing one type of the groups (A or B) is progressively fortified or locally immobilized with each already formed row of links. The relative motion of groups A and B is thus further restricted from one side, thus increasing the effective equilibrium constant.

Beyond some limit of the chain length or sheet width, the proximity effect probably remains the same. The values of both ξ_k and σ_j can thus be expected to converge to some maximum value.

In our mathematical model, we assume for simplicity that both complementary polymers have the same number $2n$ of groups A or B and that n is large enough so that we can ignore end effects without gross imprecision. We denote the equilibrium concentrations of the groups A and B as [A] and [B], respectively, with $[A]_0$ and $[B]_0$ being the respective initial concentrations. We further define the ratio $\beta = [A]_0/[B]_0$, $\beta \in \langle 0,1 \rangle$ and the turnover of the reactant groups of A, $\alpha = 1 - [A]/[A]_0$. Thus, $[A] = [B]_0\beta(1 - \alpha)$ and $[B] = [B]_0(1 - \alpha\beta)$.

The polymer coupling products can be symbolized as matrixes with a virtually infinite number of rows and n columns, with the matrix elements 1 if the corresponding link exists and 0 otherwise. To make the notation less cumbersome, we symbolize these matrixes as $\mathbf{P}_{j,k}$, where all first $(j - 1)$ rows and k first elements of the jth row uniformly contain 1 and the rest contain 0. In agreement with our above assumptions, we can write for the concentrations of the corresponding products

$$[\mathbf{P}_{1,1}] = \frac{K[A][B]}{(2n)^2} \tag{4}$$

$$[\mathbf{P}_{1,n}] = \frac{KK_1^{n-1}[A][B]^{n-1}}{(2n)^2}\prod_{i=1}^{} \xi_i \tag{5}$$

$$[\mathbf{P}_{2,2}] = \frac{K^2 K_1{}^n [\mathrm{A}]^2 [\mathrm{B}]}{(2n)^3} \sigma_1 \xi_1 \prod_{i=1}^{n-1} \xi_i \quad (6)$$

and, generally (after expressing [A] and [B] in $[\mathrm{B}]_0$, β, and α),

$$[\mathbf{P}_{j,k}] = \frac{K^j K_1{}^{(j-1)n+k-1} [\mathrm{B}]_0{}^{2j+1} [\beta(1-\alpha)]^{j+r} [1-\alpha\beta]^{j+s}}{(2n)^{j+1}} \sigma_{j-1}{}^{k-1} \prod_{i=1}^{j-2} \sigma_i{}^{n-1} \prod_{i=1}^{k-1} \xi_i \prod_{i=1}^{n-1} \xi_i{}^{j-1} \quad (7)$$

where r and s are 1 and 0 (for j even) or 0 and 1 (for j odd), respectively. Equations 4−7 describe only half of the model, in the same way Scheme 1 does. In reality, the attachments can proceed in a mirror manner starting from the second row in Scheme 1, only with A substituted by B and vice versa. Thus, the turnover α, which is our chief experimental indicator of cooperativity, can be expressed:

$$\alpha = \{\sum_{k=1}^{n} k[\mathbf{P}_{1,k}] + 2\sum_{j=2}^{\infty}\sum_{k=1}^{n}[(j-1)n+k][\mathbf{P}_{jk}]\}/[\mathrm{A}]_0 \quad (8)$$

Equation 8 is an implicit equation as $[\mathbf{P}_{jk}]$ contains α. Therefore, it has to be solved numerically, with $[\mathrm{A}]_0$, $[\mathrm{B}]_0$, and all the values of σ_i and ξ_i being the input constants and α being the optimized variable. In the second term of eq 8, the first summation has to be stopped at some reasonable value; we do it at $j = m$ if $[\mathbf{P}_{m-1,n}] < 10^{-5} \times [\mathbf{P}_{1,n}]$.

For the development of the cooperativity factors ξ_i and σ_j, we assume the sufficiently flexible logistic functions

$$\xi_i = \frac{\xi_1 - \xi_{\max}}{1 + (i/q)^p} + \xi_{\max} \quad (9)$$

and

$$\sigma_j = \frac{\sigma_1 - \sigma_{\max}}{1 + (j/q)^p} + \sigma_{\max} \quad (10)$$

where ξ_1, $\xi_{\max}$ and σ_1, $\sigma_{\max}$ are the lower and upper bounds of ξ and σ, respectively, and p and q are factors determining the form of the dependence (q is near to its inflection point, and p determines the steepness of increase).

A computer program was written by us solving eq 8 (with the use of eqs 7, 9, and 10) by a modified Newton method minimizing the change of α between two consecutive iteration steps. The model is too cumbersome to fit its parameters to the experimental points but can be used for a near-as-possible simulation.

In the following simulations, we assume $\xi_1 = \sigma_1 = 10$, $\xi_{\max} = \sigma_{\max} = 40$, $q = 20$, and $p = 2.5$. The starting concentration $[\mathrm{B}]_0$ was assumed to be 0.1 mol/L, β was incremented from 0.2 to 1.0 for each n, which was increased from 5 to 80. The equilibrium constant K was assumed to be the same as that of the binding of monomeric pyridine to PVF, that is, 5.3 mol^{-1} L^{-1} (cf. ref 37). K_1 for simplicity was assumed to be equal to 1.0.

The illustrative simulations for these constants are shown in Figure 8. As one can see, the model offers dependences of α on both n and β, very similar to those obtained in our experiments. This similarity cannot be taken as a proof of the validity of the proposed mechanism of *two-dimensional* cooperativity in our actual case, it only illustrates the feasibility of its interpretation from the quantitative point of view.

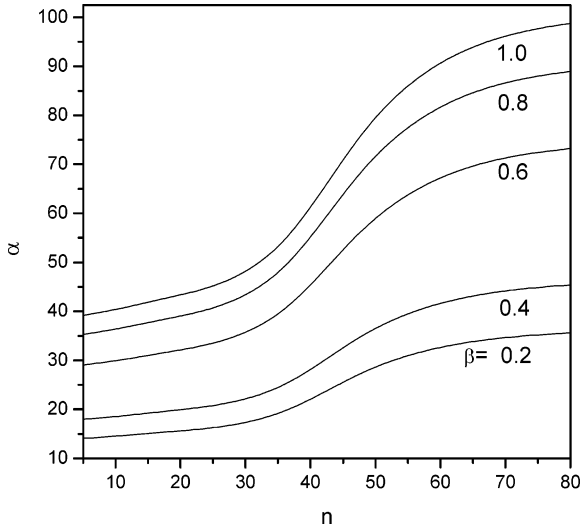

Figure 8. Simulation of the binding degree α of the polymer A in a two-dimensionally cooperative binding with B on its chain length n under various ratios $\beta = [\mathrm{A}]_0/[\mathrm{B}]_0$.

Conclusions

We have shown that PVP binds cooperatively to PVF, thus substituting its original H-bonded ligand pyridine. The cooperativity of this interaction is of a higher order, that is, exhibiting a sigmoidal dependence of the binding degree α on the chain length of PVP. In addition, it is also two-dimensional, that is, exhibiting a somewhat less pronounced sigmoidal dependence of α on the molar ratio of PVP to PVF. The explanation of this behavior appears to be in the nature of the product, which, according to our results, forms a two-dimensional polymer sheet with intermittent H-bond links between PVF and PVP chains. The main source of the found cooperativity probably is in the proximity effect of the already formed links restricting the relative positions and conformations of the chain segments bearing the remaining free reactant groups and thus lowering the entropy loss caused by the subsequent coupling. Another factor supporting the cooperativity is the entropy gain of the ligand pyridine molecules liberated by their substitution for the pyridine groups of PVP.

Acknowledgment. The authors thank the Grant Agency of the Academy of Sciences of the Czech Republic for financial support given under the Grant IAA 400500604.

References and Notes

(1) Lehn, J.-M. *Supramolecular Chemistry*; VCH Publishers: Weinheim, Germany, 1995.

(2) Tsuchida, E. *Macromolecular Complexes, Dynamic Interactions and Electronic Processes*; VCH Publishers: New York, 1991.

(3) Mich, J., Ed. *Modular Chemistry*; Proceedings, NATO ASI Series, Series C; Kluwer Academic Publishers: Norwell, MA, 1997; Vol. 49.

(4) Weber, A., Ed. *Structure and Dynamics of Weakly Bound Molecular Complexes*; Kluwer Academic Publishers: Norwell, MA, 1987.

(5) Pimentel, G. C.; McClellan, A. L. *The Hydrogen Bond*; W. H. Freeman and Co.: San Francisco/New York, 1960.

(6) Desiraju, G. R.; Steiner, T. *The Weak Hydrogen Bond*; Oxford University Press: Oxford, 1999.

(7) Otero, R.; Schock, M.; Molina, L. M.; Laegsgaard, E.; Stensgaard, I.; Hammer, B.; Besenbacher, F. *Angew. Chem. Int. Ed.* **2005**, *44*, 2270.

(8) Tolstoy, P. M.; Schah-Mohammedi, P.; Smirnov, S. N.; Golubev, N. S.; Denisov, G. S.; Limbach, H. H. *J. Am. Chem. Soc.* **2004**, *126*, 5621.

(9) Arno, M.; Domingo, L. R. *Org. Biomol. Chem.* **2003**, *1*, 637.

(10) Fraile, A. G.; Morris, D. G.; Martinez, A. G.; Cerero, S. D.; Muir, K. W.; Ryder, K. S.; Vilar, E. T. *Org. Biomol. Chem.* **2003**, *1*, 700.

(11) Hawley, J.; Bampos, N.; Aboitiz, N.; Jimenez-Barbero, J.; de la Paz, M. L.; Sanders, J. K. M.; Carmona, P.; Vicent, C. *Eur. J. Org. Chem.* **2002**, *12*, 1925.

(12) Ng, S. W.; Naumov, P.; Chantrapromma, S.; Raj, S. S. S.; Fun, H. K.; Ibrahim, A. R.; Wojciechowski, G.; Brzezinski, B. *J. Mol. Struct.* **2001**, *569*, 139.

(13) Hoffmann, M.; Rychlewski, J. *J. Am. Chem. Soc.* **2001**, *123*, 2308.

(14) Prins, L. J.; De Jong, F.; Timmerman, P.; Reinhoudt, D. N. *Nature* **2000**, *408*, 181.

(15) Zhou, J.; He, X. W.; Guo, H. S. *Chin. J. Chem.* **2000**, *18*, 482.

(16) Gabius, H. J. *Naturwissenschaften* **2000**, *87*, 108.

(17) Lipkowski, P.; Bielejewska, A.; Kooijman, H.; Spek, A. L.; Timmerman, P.; Reinhoudt, D. N. *Chem. Commun.* **1999**, *14*, 1311.

(18) Kirsten, C. N.; Schrader, T. H. *J. Am. Chem. Soc.* **1997**, *119*, 12061.

(19) Sijbesma, R. P.; Beijer, F. H.; Brunsveld, L.; Folmer, B. J. B.; Hirschberg, J. H. K.; Lange, R. F. M.; Lowe, J. K. L.; Meijer, E. W. *Science* **1997**, *278*, 1601.

(20) Doseva, V.; Shenkov, S.; Baranovsky, V. Y. *Polymer* **1997**, *38*, 1339.

(21) Ng, K. K. S.; Weis, W. I. *Biochemistry* **1997**, *36*, 979.

(22) Steiner, T.; Saenger, W. *J. Am. Chem. Soc.* **1992**, *114*, 114.

(23) Spange, S.; Heinze, T.; Klemm, D. *Polym. Bull.* **1992**, *28*, 697.

(24) Kříž, J.; Kurková, D.; Dybal, J.; Oupick×c6, D. *J. Phys. Chem. A* **2000**, *104*, 10972.

(25) Kříž, J.; Dautzenberg, H. *J. Phys. Chem. A* **2001**, *105*, 3846.

(26) Kříž, J.; Dybal, J.; Dautzenberg, H. *J. Phys. Chem. A* **2001**, *105*, 7486.

(27) Kříž, J.; Dybal, J.; Kurková, D. *J. Phys. Chem. B* **2002**, *106*, 2175.

(28) Kříž, J.; Dybal, J.; Kurková, D. *J. Phys. Chem. A* **2002**, *106*, 7971−7981.

(29) Kříž, J.; Dautzenberg, H.; Dybal, J.; Kurková, D. *Langmuir* **2002**, *18*, 9594.

(30) Kříž, J.; Dybal, J.; Kurková, D. *J. Phys. Chem. B* **2003**, *107*, 12165.

(31) Stejskal, E. O.; Tanner, J. E. *J. Chem. Phys.* **1965**, *42*, 288.

(32) Tanner, J. E. *J. Chem. Phys.* **1970**, *52*, 2523.

(33) van Rossum, B. J.; de Groot, C. P.; Ladizhansky, V.; Vega, S.; de Groot, H. J. M. *J. Am. Chem. Soc.* **2000**, *122*, 3465.

(34) van Rossum, B. J.; Schulten, E. A. M.; Raap, J.; Oschkinat, H.; de Groot, H. J. M. *J. Magn. Reson.* **2002**, *155*, 1.

(35) Bennet, A. E.; Rienstra, C. M.; Auger, M.; Lakshmi, K. V.; Griffin, R. G. *J. Chem. Phys.* **1995**, *103*, 6951.

(36) Frisch, M. J.; Trucks, G. W.; Schlegel, H. B.; Scuseria, G. E.; Robb, M. A.; Cheeseman, J. R.; Montgomery, J. A., Jr.; Vreven, T.; Kudin, K. N.; Burant, J. C.; Millam, J. M.; Iyengar, S. S.; Tomasi, J.; Barone, V.; Mennucci, B.; Cossi, M.; Scalmani, G.; Rega, N.; Petersson, G. A.; Nakatsuji, H.; Hada, M.; Ehara, M.; Toyota, K.; Fukuda, R.; Hasegawa, J.; Ishida, M.; Nakajima, T.; Honda, Y.; Kitao, O.; Nakai, H.; Klene, M.; Li, X.; Knox, J. E.; Hratchian, H. P.; Cross, J. B.; Bakken, V.; Adamo, C.; Jaramillo, J.; Gomperts, R.; Stratmann, R. E.; Yazyev, O.; Austin, A. J.; Cammi, R.; Pomelli, C.; Ochterski, J. W.; Ayala, P. Y.; Morokuma, K.; Voth, G. A.; Salvador, P.; Dannenberg, J. J.; Zakrzewski, V. G.; Dapprich, S.; Daniels, A. D.; Strain, M. C.; Farkas, O.; Malick, D. K.; Rabuck, A. D.; Raghavachari, K.; Foresman, J. B.; Ortiz, J. V.; Cui, Q.; Baboul, A. G.; Clifford, S.; Cioslowski, J.; Stefanov, B. B.; Liu, G.; Liashenko, A.; Piskorz, P.; Komaromi, I.; Martin, R. L.; Fox, D. J.; Keith, T.; Al-Laham, M. A.; Peng, C. Y.; Nanayakkara, A.; Challacombe, M.; Gill, P. M. W.; Johnson, B.; Chen, W.; Wong, M. W.; Gonzalez, C.; Pople, J. A. *Gaussian 03*, revision C.02; Gaussian, Inc.: Wallingford, CT, 2004.

(37) Kříž, J.; Dybal, J. *J. Phys. Chem. B* **2005**, *109*, 13436−13444.

(38) Schmidt-Rohr, K.; Clauss, J.; Spiess, H. W. *Macromolecules* **1992**, *25*, 3273.

(39) Jia, X.; Wolak, J.; Wang, X.; White, J. L. *Macromolecules* **2003**, *36*, 712.